Influence of the cooling rate on the glass transition temperature and the structural properties of glassy GeS_2: an *ab initio* molecular dynamics study

2007 J. Phys.: Condens. Matter 19 196102

(http://iopscience.iop.org/0953-8984/19/19/196102)

IOP PUBLISHING JOURNAL OF PHYSICS: CONDENSED MATTER

J. Phys.: Condens. Matter **19** (2007) 196102 (11pp) doi:10.1088/0953-8984/19/19/196102

Influence of the cooling rate on the glass transition temperature and the structural properties of glassy GeS_2: an *ab initio* molecular dynamics study

Sébastien Le Roux and Philippe Jund

Laboratoire de Physicochimie de la Matière Condensée—Institut Charles Gerhardt, Université Montpellier 2, Place E. Bataillon, Case 03, 34095 Montpellier, France

Received 26 September 2006, in final form 14 March 2007
Published 17 April 2007
Online at stacks.iop.org/JPhysCM/19/196102

Abstract

Using density-functional molecular dynamics simulations we analysed the effects of the cooling rate on the physical properties of GeS_2 chalcogenide glasses. Liquid samples were cooled linearly in time according to $T(t) = T_0 - \gamma t$ where γ is the cooling rate. We found that our model leads to a promising description of the glass transition temperature T_g as a function of γ and gives a correct T_g for experimental cooling rates. We also investigated the dependence of the structural properties on the cooling rate. We show that, globally, the properties determined from our simulations are in good agreement with experimental values, even for the highest cooling rates. In particular, our results confirm that, in the range of cooling rates studied here, homopolar bonds and extended charged regions are always present in the glassy phase. Nevertheless, in order to reproduce the experimental intermediate range order of the glass, a maximum cooling rate should not be exceeded in numerical simulations.

(Some figures in this article are in colour only in the electronic version)

1. Introduction

During the last 15 years the steadily growing interest in chalcogenide glasses has led to numerous works. This is true in particular for germanium disulfide glasses for which a large number of experimental [1–4] and theoretical [5–8] studies have been carried out. Indeed its known properties—used, for example, in optical amplifiers, memory switching devices and anti-reflection coatings [9]—make it a good candidate for intensive research.

Among the different research methods, molecular dynamics (MD) simulations are a very interesting tool for providing detailed information on the physical properties of such glassy systems. Firstly because they allow one to investigate the structure in full microscopic detail giving access to the position of the atoms, and secondly because they are useful for studying

dynamic phenomena accessible to such simulations, e.g. for timescales between 10^{-13} and 10^{-8} s.

If the temperature of a liquid is decreased so much that the relaxation time of the system becomes longer than the timescale of the computer simulation or of the experiment, the system undergoes a kinetic arrest and, provided that it does not crystallize, will undergo a glass transition and remain trapped in a disordered configuration. However, it has been demonstrated in both experiment [10, 11] and computer simulations [12, 13] that the properties of the resulting glass, like the density or the glass transition temperature, will depend on its thermal history and in particular on the rate at which the sample is cooled down.

Previous studies [5–7] have already validated our 'cook and quench' model to produce and study GeS_2 glasses using approximate *ab initio* molecular dynamics simulations. Nevertheless, because of the timescale of our computer simulations, which is many orders of magnitude shorter than the typical experimental one, the glass transition temperature, for example, appears to be significantly higher than the one observed in the laboratory (∼750 K [2, 14, 15]), and thus it is necessary to see how the properties of the so-obtained glass depend on the way in which it was produced.

Thus in the present paper we focus on the effects of the cooling rate on some physical properties of glassy GeS_2. Firstly we investigate how cooling rate affects the glass transition temperature T_g and secondly we study how it affects the structural properties of the glassy samples.

The paper is consequently organized as follows. In section 2 we briefly present the theoretical model used in our calculations, results and discussions are presented in section 3, and finally in section 4 we summarize the major conclusions of our work.

2. Theoretical framework

Computations were performed using Fireball96, an approximate *ab initio* molecular dynamics code based on the local-orbital electronic structure method developed by Sankey and Niklewski [16]. The electronic structure is described using density functional theory (DFT) [17] within the local density approximation (LDA) [18] and the non-local pseudo-potential scheme of Bachelet, Hamann and Schlüter [19]. To reduce the CPU time we used the non-self-consistent Harris functional [20] with a set of four atomic orbitals (one 's' and three 'p') per atom that vanish outside a cut-off radius of $5a_0$ (2.645 Å). This model has been successfully used for the last 10 years for several different chalcogenide systems [5–7, 21–23].

All the calculations of the present simulations were performed in the microcanonical ensemble, with a time step $\Delta t = 2.5$ fs and using only the Γ point to sample the Brillouin zone. The initial configuration of our system was a crystal of α-GeS_2 in a cubic cell of 19.21 Å containing 258 atoms with standard periodic boundary conditions, melted at 2000 K for 60 ps in order to obtain an equilibrium liquid. Then, we relaxed this system further at 2000 K for 50 ps and we chose five different liquid samples (approximately every 10 ps) during this process. Each sample was then quenched down to 300 K through the glass transition temperature T_g. Quenches were carried out by a linear velocity rescaling according to $T(t) = T_0 - \gamma t$, where γ is the cooling rate. Six different cooling rates were used: 3, 0.6, 0.3, 0.12, 0.09 and 0.06×10^{14} K s^{-1}. At 300 K each sample was relaxed over 50 ps, i.e. 20 000 time steps. Configurations were saved every 20 steps and the results were averaged for each sample over these 1000 configurations. Furthermore we averaged the results for the five samples of each cooling rate, thus all the data presented below have been averaged over 5×1000 configurations, and the error bars (when given) represent the usual standard deviation.

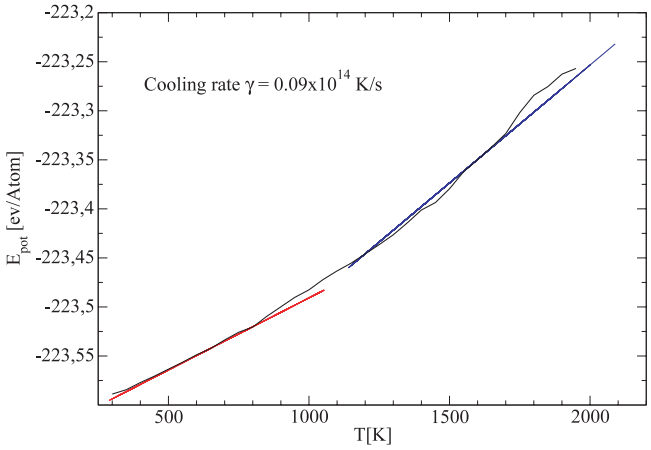

Figure 1. Average potential energy as a function of the temperature and linear regressions above and below the glass transition temperature for a sample cooled at 0.09×10^{14} K s^{-1}.

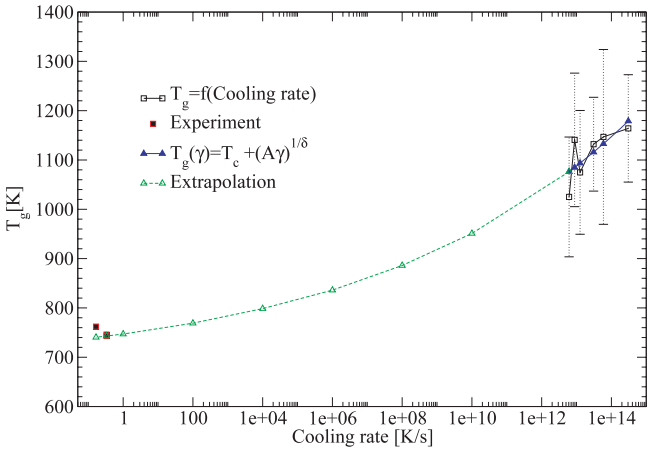

Figure 2. Glass transition temperature as a function of the cooling rate, fit and extrapolation to very low cooling rates—comparison with experiment [2, 14, 15].

3. Results

3.1. Glass transition

As is usually done in simulations we tried to identify the glass transition of our samples by representing the evolution of the average potential energy as a function of the temperature during the quench (an example is proposed for one of the samples cooled at 0.09×10^{14} K s^{-1} (figure 1)), the glass transition being localized by the change in the evolution of the energy. The glass transition temperature T_g is determined by the intersection of the two linear regressions at high and low temperature (figure 1). For each cooling rate we averaged the values of the T_g obtained for each of the five GeS_2 samples, and thus we obtained an evolution of the average T_g with the cooling rate. As shown in figure 2 the error bars remain huge, indicating insufficient sampling (it is worth noting that the computer time needed to perform the simulations for the lowest values of γ is of the order of 12 weeks for one sample) and it is therefore difficult to

extract an accurate description of the evolution of T_g with the cooling rate. Nevertheless we attempted to fit these average simulation values assuming a power-law dependence of T_g with the cooling rate as suggested by the mode-coupling theory [24]:

$$T_g(\gamma) = T_c + (A\gamma)^{1/\delta} \tag{1}$$

with $T_c = 676 \pm 75$ K, $A = 3.0 \pm 2.3 \times 10^{31}$ and $\delta = 17.1 \pm 0.1$ (the errors given for the parameters of the fit have been evaluated by fitting the extreme (lowest and highest) T_g values enclosed in the error bars). We observed that a variation of γ by about 1 decade gives rise to a variation of T_g of about 75 K which is not much larger, compared to the difference of magnitude of the cooling rates, than the variation of 10 K measured in real experiments for different materials [10, 11, 24]. Then by extrapolating the results of our fit down to the usual experimental cooling rates, i.e. 10^0–10^5 K s^{-1}, we observed at this scale that a variation of γ by about 1 decade gives rise to a variation of T_g of about 13 K, which is in agreement with the experimental variation of 10 K previously mentioned. We have represented in figure 2 the result of this work together with a few experimental data [2, 14, 15]. The agreement between the extrapolation of the fit and the experimental values of T_g shows that our model is able to give a correct *tendency* of the variation of T_g with γ, even though the poor statistics prevents us from having accurate estimates of T_g at a specific (high) cooling rate. This can be improved with more simulations in order to reduce the error bars.

3.2. Structural properties

3.2.1. Radial pair correlation functions and bonding properties. In glassy GeS_2 the basic building blocks are GeS_4 tetrahedra, connected together to form a random network. The structural disorder is reflected by the absence of long-range order and by the wide distribution of bond lengths and bond angles. Structural information may be extracted from the radial pair correlation function $g(r)$ which can be defined for a given α, β pair by:

$$g_{\alpha\beta}(r) = \frac{V}{4\pi r^2 \rho N c_\alpha c_\beta} \sum_{i \neq j} \delta(r - r_{ij}) \tag{2}$$

where ρ is the number density of the system, c_α the fraction of species α in the system, i the atoms of species α and j the atoms of species β. For each cooling rate we averaged the radial pair correlation functions $g_{\alpha\beta}(r)$ of the five samples, so we are able to compare the evolution of the average $g_{\alpha\beta}(r)$ according to the cooling rate (figures 3 and 4).

The bond lengths appear to be in good agreement with experimental data [2] since we find 2.23 Å for the Ge–S bond (expe.: 2.21 Å), 2.91 and 3.49 Å for respectively the edge and corner sharing Ge–Ge connections (expe: 2.91 and 3.42 Å). This good agreement is true even for the highest cooling rates. The main influence of the cooling rate is reflected in the small peak corresponding to homopolar bonds between 2.2 and 2.6 Å for Ge (figure 3) and 2.1 and 2.45 Å for S (figure 4). Our results indicate that the number of homopolar bonds decreases with the cooling rate and it is therefore justified to address the question of the existence of homopolar bonds at experimental cooling rates which is still an open question (Cai and Boolchand, using a Raman scattering experiment, showed the existence of homopolar bonds in glassy GeS_2 [25] while Petri and Salmon found no evidence of such bonds in $g GeS_2$ using neutron diffraction [14] studies). According to figures 3 and 4 it seems that the decrease of the proportion of homopolar bonds slows down for the lowest cooling rates and tends towards a limit of 1.9% for the Ge atoms and 1.2% for the S atoms. These limiting values are small but nonzero, and therefore our simulation results seem to confirm the existence of homopolar bonds in experimental glassy GeS_2.

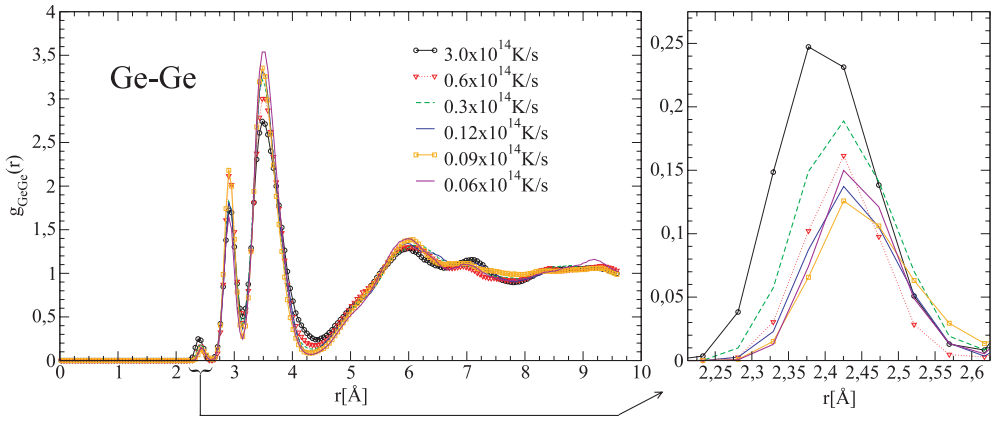

Figure 3. Partial radial pair distribution function $g(r)$ [Ge–Ge] as a function of the cooling rate. Enlargement corresponds to details of the peak due to homopolar bonds.

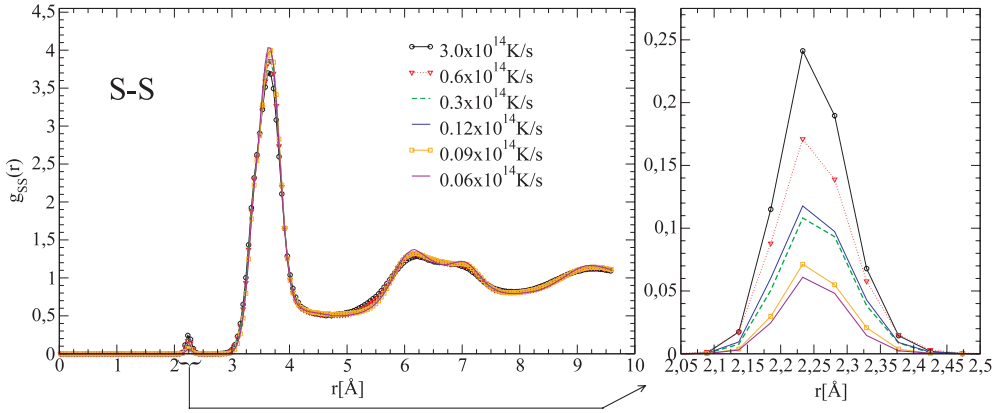

Figure 4. Partial radial pair distribution function $g(r)$ [S–S] as a function of the cooling rate. Enlargement corresponds to details of the peak due to homopolar bonds.

The simulation gives access to the positions of the atoms; therefore we can also obtain information on the connectivity of the network. In our approach we focused on the ratio between edge and corner sharing tetrahedra and the evolution of the different local environments of the Ge (table 1) and S atoms (table 2).

First it is worth noting that the proportion of edge- and corner-sharing links is almost a constant independent of the cooling rate: 84% $\pm$ 1.8 of corner-sharing and 16% $\pm$ 1.8 of edge-sharing bounds, values in good agreement with experimental data [2]. This is in contrast with the evolution of the proportions of germanium (table 1) and sulfur (table 2) in their standard environment (respectively a four-fold S coordination for Ge and a two-fold Ge coordination for S) which increase appreciably with decreasing cooling rate. The second point concerns, as expected, the decrease of the chemical disorder with decreasing cooling rate. Indeed the proportion of under-coordinated Ge atoms (2.3% for the fastest cooling rate) disappears for the slowest cooling rate. And the proportions of non-bridging S atoms and over-coordinated S atoms, respectively 14.25% and 12.85%, decrease to 10.4% and 9.8%.

Table 1. Evolution of the local structural environment of Ge atoms as a function of the cooling rate γ.

	Proportion of Ge atoms (%)		
γ (10^{14} K s^{-1})	**Ge**(S_4)	**Ge**(S_3)	**Ge**(GeS_3)
3	93.0 ± 2.0	2.3 ± 1.8	3.7 ± 2.1
0.6	95.0 ± 1.6	1.7 ± 1.1	1.9 ± 2.0
0.3	96.2 ± 1.8	0.3 ± 0.3	2.8 ± 2.0
0.12	96.4 ± 1.8	1.7 ± 1.8	1.9 ± 2.0
0.09	97.6 ± 1.7	0.1 ± 0.1	1.8 ± 1.0
0.06	98.1 ± 1.0	0.0 ± 0.0	1.9 ± 1.1

Table 2. Evolution of the local structural environment of S atoms as a function of the cooling rate γ.

	Proportion of S atoms (%)				
γ (10^{14} K s^{-1})	**S**(Ge_2)	**S**(Ge)	**S**(Ge_3)	**S**(GeS)	**S**(Ge_2S)
3	67.9 ± 2.2	14.3 ± 1.5	12.9 ± 1.8	3.1 ± 1.3	1.8 ± 0.9
0.6	71.0 ± 4.1	12.9 ± 2.0	12.6 ± 1.8	2.1 ± 0.8	0.4 ± 0.3
0.3	75.5 ± 2.6	11.4 ± 1.0	10.7 ± 1.2	2.0 ± 1.3	0.4 ± 0.6
0.12	76.1 ± 2.7	10.9 ± 1.2	10.5 ± 1.3	1.7 ± 0.8	0.6 ± 0.6
0.09	78.2 ± 3.3	10.4 ± 1.6	9.9 ± 1.4	1.1 ± 1.1	0.4 ± 0.3
0.06	78.5 ± 1.0	10.4 ± 0.4	9.8 ± 1.0	0.8 ± 0.3	0.4 ± 0.3

These results indicate that the cooling rate has an impact on the structure of the glass. Nevertheless while certain types of structural 'defects' disappear at low cooling rates, others survive and can therefore be considered as inherent to the glassy structure.

3.2.2. Static neutron structure factor. An alternative way to analyse the structure is to compute the static neutron structure factor $S(q)$ which can be directly compared to neutron scattering experiments:

$$S(q) = \frac{1}{N} \sum_{j,k} b_j \, b_k \langle e^{iq[r_j - r_k]} \rangle \tag{3}$$

where N is the number of atoms and b_j is the neutron scattering factor for atom j.

As for the radial pair distribution functions, we averaged for each cooling rate the total neutron structure factors of the five samples, thus permitting a comparison of the evolution of the average structure factors as a function of the cooling rate (figure 5).

First we note the accurate description of glassy GeS_2 reflected in the good agreement between the simulated curves and the experimental one, even for the highest cooling rates. Although the simulated and experimental curves present differences in the range 0–2.5 Å^{-1} it has already been shown [6, 7, 26] that the physical properties of the so-simulated glassy samples are in good agreement with experiment. The first sharp diffraction peak (FSDP), the signature of the intermediate-range order (IRO) in amorphous samples, appears at $\approx$1 Å^{-1} and is, as expected in such simulations, slightly underestimated [5]. Size effects can be considered as an explanation, nevertheless we note that a decrease in the cooling rate globally improves the calculated structure factor and in particular the FSDP (figure 5), which highlights that the

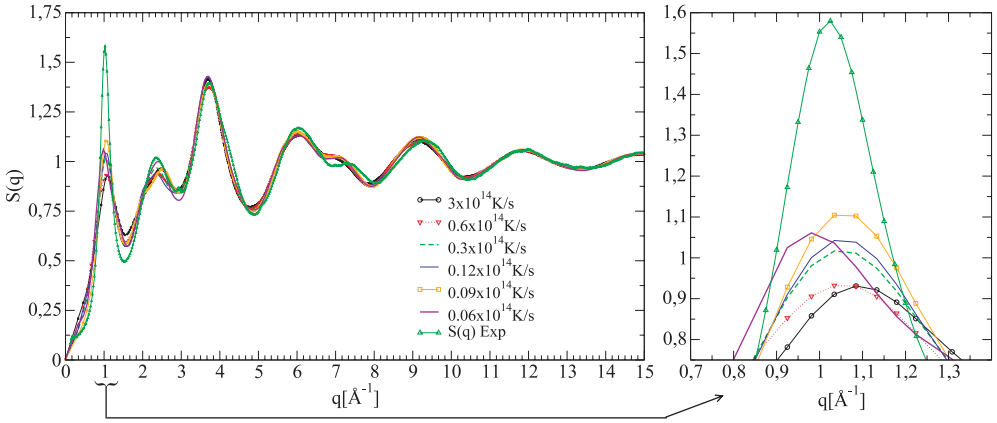

Figure 5. Total simulated static neutron structure factors. Enlargement corresponds to the FSDP part of the $S(q)$.

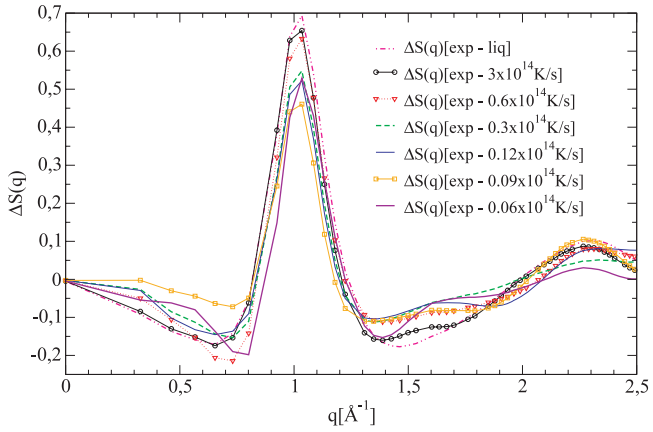

Figure 6. $\Delta S(q)$ for the IRO, between experiment and liquid GeS_2, and between experiment and glassy GeS_2 for the different cooling rates.

IRO is also dependent on cooling rate. However, there is no linear/regular evolution of $S(q)$ with cooling rate. To illustrate the improvement of $S(q)$ in the FSDP region with the decrease in the cooling rate, we represent (in figure 6) the difference, between 0 and 2.5 Å^{-1}, of the experimental total neutron structure factor and:
(1) the total neutron structure factor of the liquid state at 2000 K:

$$S(q)_{\mathrm{exp}} - S(q)_{\mathrm{liq}} = \Delta S(q)_{\mathrm{exp-liq}}$$

(2) the average total neutron structure factor of the simulated glass quenched down to 300 K at the rate γ:

$$S(q)_{\mathrm{exp}} - S(q)_{\gamma} = \Delta S(q)_{\mathrm{exp}-\gamma}.$$

$\Delta S(q)_{\mathrm{exp-liq}}$ is a reference representing the biggest variation between the experimental and simulated $S(q)$ and should be compared to $\Delta S(q)_{\mathrm{exp}-\gamma}$. We see in figure 6 that by decreasing the cooling rate the difference $\Delta S(q)_{\mathrm{exp}-\gamma}$ decreases. In particular it appears that for cooling

Table 3. Löwdin charges according to the local structural environments in an equilibrium liquid GeS_2 at 2000 K.

Environment	q	Proportion (%)
Ge(S_4)	$+0.96 \pm 0.04$	64.83
Ge(S_3)	$+1.02 \pm 0.06$	27.41
Ge(GeS_3)	$+0.75 \pm 0.1$	1.14
Ge–**S**–Ge	-0.43 ± 0.15	60.22
Ge–**S**	-0.92 ± 0.21	26.03
$\overset{\text{Ge}}{\text{Ge}}$ > **S**-Ge	-0.03 ± 0.11	9.74
Ge–**S**–S	-0.1 ± 0.18	2.07
$\overset{\text{Ge}}{\text{Ge}}$ > **S**–S	0.32 ± 0.2	1.60

rates higher than 0.3×10^{14} K s^{-1} the differences $\Delta S(q)_{\text{exp}-\gamma}$ are very close to the difference $\Delta S(q)_{\text{exp}-\text{liq}}$. For the highest cooling rate (3×10^{14} K s^{-1}) this difference is even quasi identical to $\Delta S(q)_{\text{exp}-\text{liq}}$ which indicates that there is no real change in the IRO between the fastest quenched glass and the liquid phase. One can thus argue that the fastest cooled samples are too similar to the liquid and cannot therefore be considered as glassy GeS_2 samples. This defines a limit for the maximum cooling rate usable in MD simulations in order to avoid interferences between the liquid and the glassy state. In our simulations this limit appears to be between 0.6×10^{14} K s^{-1} and 0.3×10^{14} K s^{-1}. Nevertheless this limit is directly related to the method, i.e. *ab initio* MD simulations, and indirectly related to our model, i.e. the nature of the glass and the characteristics of the atomic pseudopotentials, and therefore the numerical value of this limit cannot be straightforwardly extended to other simulated glassy systems.

3.2.3. Atomic charges. Even if atomic charges cannot actually be determined experimentally, relevant tools such as Löwdin [27] or Mulliken [28] population analysis can be used to compare different configurations with the *same* description. In the present work the Löwdin description has been chosen in order to compare the dependence of the atomic charges on the cooling rate. However, it should be mentioned that the non-self-consistent Harris functional is known to overestimate the charge transfers between the atoms.

The atomic charge q is calculated by the difference between the number of electrons of the neutral atom and the 'real' number of electrons of the atom in the glass. We found no dependence of the Löwdin charges on the cooling rate. Thus it is necessary to correlate the charges with the evolution of the proportion of each atomic type in its local structural environment with the cooling rate (tables 1 and 2).

As expected, the general polarity of the Ge–S bond is found with a charge transfer in an ordered $Ge(S_4)_{1/2}$ configuration of $+0.94$ for the Ge atoms and -0.46 for the S atoms. As has already been shown in a previous work [6] Ge charges are always positive and decrease with the number of neighbours, whereas S charges are more variable with respect to the local environment: from strongly negative charges for non-bridging S atoms (-1.07) to almost neutral charges for three-fold Ge-coordinated S atoms. And even if the existence of positively charged S atoms in the environment $\overset{\text{Ge}}{\text{Ge}}$ > S-S is confirmed in our present work, table 2 shows that this kind of local structural environment disappears rapidly with decreasing cooling rate. These structures obtained at high cooling rate may be explained by the results shown in table 3, representing the charge of an atom in a given local structural environment and the proportion of atoms in this environment in an equilibrium GeS_2 liquid at 2000 K. Indeed it appears that the configuration of the liquid is quite similar, at least for the S atoms, to the fastest cooled glass configurations (table 2). This result indicates that the fastest cooled glasses are, in the

Table 4. Evolution of the average number of charged zones as a function of the cooling rate γ.

	Averaged number of charged zones	
γ (10^{14} K s^{-1})	$\Delta Q_{SR} > +0.3$	$\Delta Q_{SR} < -0.3$
3	9.0 ± 1.0	20.8 ± 1.2
0.6	9.0 ± 2.0	19.2 ± 0.8
0.3	8.4 ± 1.6	17.2 ± 0.8
0.12	8.6 ± 1.4	16.0 ± 1.0
0.09	7.8 ± 1.8	15.8 ± 0.2
0.06	9.2 ± 0.8	16.4 ± 0.6

literal sense, frozen liquids. This confirms what we have already detected in the total neutron structure factor.

Positively and negatively charged zones inside the glass have been reported in our previous study [6] for the highest cooling rate. In order to see if the atomic charges measured for the lowest cooling rate confirm or reject the existence of such zones we looked at the short-range charge deviation ΔQ_{SR} of a particle i defined by:

$$\Delta Q_{SR}(i) = q(i) + \sum_{j=1}^{n(i)} \frac{q(j)}{n(j)}. \tag{4}$$

This allows us to take into account the atomic charge $q(i)$ of a given particle i as well as the charges on its $n(i)$ nearest neighbours (determined from the radial pair distribution function). Whereas for a crystalline structure, in which no bond defects are present, this value is almost zero for all the particles, positive and negative values appear for glassy samples.

In table 4 we have reported the evolution of the number of charged zones (a charged zone contains at least two nearest neighbours having the same sign for ΔQ_{SR}) as a function of the cooling rate.

The number of positively charged zones (particles with $\Delta Q_{SR} > +0.3$) is almost constant and equal to 9, with no dependence on the cooling rate, whereas the number of negatively charged zones (particles with $\Delta Q_{SR} < -0.3$) decreases slightly from ∼20 for samples cooled at 3×10^{14} K s^{-1} to ∼16 for samples cooled at a rate less than 0.3×10^{14} K s^{-1} (this is again consistent with the idea of a maximum cooling rate usable in MD simulations). The negatively charged zones are principally made of Ge atoms coordinated to one or more non-bridging sulfur atoms and, for the fastest cooled glasses, of a few S–**S**–Ge structures. As already shown (table 2) these structures disappear with decreasing cooling rate. This observation correlated with the diminution of the proportion of non-bridging sulfur atoms gives an explanation for the decrease in the number of negatively charged zones with cooling rate for rates higher than 0.3×10^{14} K s^{-1}. The positively charged zones are exclusively made of Ge atoms linked to over-coordinated S atoms.

In addition we have reported the average number of atoms per charged zone as a function of the cooling rate (table 5). This shows that the size of the positively and the negatively charged zones (with respectively five and two atoms per zone) is independent of the cooling rate and therefore remains constant. It is worth noting that the global neutrality of the glass is always respected. Our results show that the existence of charged zones in glassy GeS_2 is not influenced by the variation of the cooling rate. They thus confirm those of our previous study, and show that extended charged zones (whose manifestation has also been detected recently for other chalcogenide systems by Taraskin *et al* [29]) reflect the broken chemical order of the glass and are therefore inherent to the amorphous state.

Table 5. Evolution of the average number of atoms per charged zone as a function of the cooling rate γ.

	Average number of atoms per charged zone	
γ (10^{14} K s^{-1})	$\Delta Q_{SR} > +0.3$	$\Delta Q_{SR} < -0.3$
3	5.7 ± 0.1	2.1 ± 0.0
0.6	5.2 ± 0.4	2.1 ± 0.1
0.3	5.2 ± 1.1	2.0 ± 0.0
0.12	5.2 ± 0.2	2.1 ± 0.0
0.09	5.2 ± 1.7	2.1 ± 0.0
0.06	4.2 ± 0.2	2.1 ± 0.0

4. Conclusion

Through DFT based molecular dynamics simulations we have analysed the effect of the cooling rate on some properties of glassy GeS_2. The influence of the cooling rate on the glass transition temperature as well as on the structural properties has been studied.

Due to a lack of statistics, mainly as a result of computer time limitations (especially for the lowest cooling rates), the detailed variation of T_g with the cooling rate could not be obtained. Nevertheless the extrapolation of our results to 'realistic' cooling rates is in good agreement with the experimental glass transition temperature.

Analysing the radial pair distribution functions and the local structural environments for each cooling rate, we find that the number of S and Ge homopolar bonds as well as the number of coordination defects decrease with the cooling rate. Nevertheless the decrease in the number of homopolar bonds seems limited, and therefore it is reasonable to think that this type of defect is present in real glasses. However, calculations at lower cooling rates should be done to confirm this observation.

Study of the simulated total neutron structure factor has confirmed the reliability of our model for the description of glassy GeS_2. We have analysed the effect of the cooling rate on the intermediate-range order whose signature is the first sharp diffraction peak. The simulated FSDP is closer to the experimental one for the slowest cooled glasses. By comparison with the properties of the liquid state, we have shown that a maximum cooling rate should not be exceeded in the simulation in order to reproduce the IRO characteristic of the glassy phase. The value of this maximum cooling rate will depend on the details of the model used to describe a given system. The existence of a maximum cooling rate has also been supported by the analysis of the charges, which has revealed that the electronic configuration of the fastest cooled glasses is close to the one obtained in liquid GeS_2. In addition the existence of positively and negatively charged regions in the amorphous state has been clearly confirmed even for the lowest cooled samples and seems therefore inherent to the glassy state. These regions will have an important impact on the properties of samples containing metallic ions, as shown recently [26].

Acknowledgments

The authors wish to thank Sébastien Blaineau for his help at the beginning of this work and Annie Pradel and Benoit Coasne for profitable discussions. Parts of the calculations have been performed at the 'Centre Informatique National de l'Enseignement Supérieur'(CINES) in Montpellier.

References

[1] Hannon A C and Aitken B G 1999 *J. Phys. Chem. Solids* **60** 1473–7
[2] Boolchand P, Grothaus J, Tenhover M, Hazle M A and Grasselli R K 1986 *Phys. Rev.* B **33** 5421–34
[3] Shojiya J, Kawamoto M, Miyauchi Y, Qiu K and Kitamura N 2001 *J. Non-Cryst. Solids* **279** 186–95
[4] Philippot M, Desctes E, Ibanez L, Bionducci A and Bellissent R 1996 *J. Non-Cryst. Solids* **202** 248–52
[5] Blaineau S, Jund P and Drabold D A 2003 *Phys. Rev.* B **67** 094204
[6] Blaineau S and Jund P 2004 *Phys. Rev.* B **70** 184210
[7] Blaineau S and Jund P 2004 *Phys. Rev.* B **69** 064201
[8] Jackson K, Briley A, Grossman S, Porezag D V and Pederson M R 1999 *Phys. Rev.* B **60** R14985–9
[9] Malek J and Shanelova J 1999 *J. Non-Cryst. Solids* **243** 116–22
[10] Brüning R and Samwer K 1992 *Phys. Rev.* B **46** 11318–22
[11] Brüning R and Sutton M 1994 *Phys. Rev.* B **49** 3124–30
[12] Miyagawa H and Hiwatari Y 1989 *Phys. Rev.* A **40** 6007–13
[13] Vollmayr K, Kob W and Binder K 1996 *Phys. Rev.* B **54** 15808–27
[14] Petri L and Salmon P S 2001 *J. Non-Cryst. Solids* **202** 169
[15] Feng X, Bresser W J and Boolchand P 1997 *Phys. Rev. Lett.* **78** 4422–5
[16] Sankey O F and Niklewski D J 1989 *Phys. Rev.* B **40** 3979–95
[17] Hohenberg P and Kohn W 1964 *Phys. Rev.* **136** 864–71
[18] Kohn W and Sham L J 1965 *Phys. Rev.* **140** 1133–8
[19] Bachelet G B, Hamann D R and Schlüter M 1982 *Phys. Rev.* B **26** 4199–28
[20] Harris J 1985 *Phys. Rev.* B **31** 1770–9
[21] Li J and Drabold D A 2001 *Phys. Rev.* B **64** 104206
[22] Cobb M and Drabold D A 1997 *Phys. Rev.* B **56** 3054–65
[23] Ortega J, Pérez R and Flores F 2000 *J. Phys.: Condens. Matter* **12** L21–7
[24] Gotze W and Sjogren L 1992 *Rep. Prog. Phys.* **55** 241–376
[25] Cai L and Boolchand P 2002 *Phil. Mag.* B **82** 1649
[26] Blaineau S and Jund P 2006 *Phys. Rev.* B **74** 054203
[27] Lödin P-O 1955 *J. Chem. Phys.* **18** 365
[28] Mulliken R S 1955 *J. Chem. Phys.* **23** 1833
[29] Taraskin S N, Simdyankin S I, Elliott S R, Neilson J R and Lo T 2006 *Phys. Rev. Lett.* **97** 055504